

Quantum Imaging of Gravity

Marian Cepok,¹ Dennis Rätzel,^{1,2} and Claus Lämmerzahl^{1,2}

¹ZARM, University of Bremen, 28359 Bremen, Germany

²Gauss-Olbers Space Technology Transfer Center, University of Bremen, 28359 Bremen, Germany

We propose a quantum imaging-inspired setup for measuring gravitational fields using an atom that emits a photon at one of two possible locations. The atom acquires a gravitationally induced quantum phase that it shares with the photon. By restoring the path identity of the atom after its interaction with the gravitational field, the gravitationally induced phase can be measured using photon interferometry without the need for additional measurements on the atom. Through repeated measurements with varying interferometric setups, the gravitational potential and inertial acceleration can be deduced.

INTRODUCTION

Since its first emergence, atom interferometry has proven to be a promising instrument for measuring the gravitational field [1–3]. Today, it is recognized as one of the most precise methods not only for gravimetry [4, 5], but also for gradiometry [6], and it is already being used for tests of the equivalence principle [7–9] and local Lorentz invariance [10]. Furthermore, there are plans to detect gravitational waves using atom interferometers [11]. Atoms are ideal for high-precision measurements because atoms of the same species can be prepared identically, eliminating some sources of error and improving the reproducibility of experiments.

The indistinguishability of quantum particles also plays a central role in other types of interferometers. A notable early example is the photon-based Hong-Ou-Mandel interferometer, which demonstrates the effect of indistinguishability in quantum measurements [12], which has since been validated for atoms as well [13]. Shortly after the Hong-Ou-Mandel experiment, another interferometric setup based on the indistinguishability of photons created in a down-conversion process was proposed by Zou, Wang, and Mandel [14]. This setup later became the foundation of Quantum Imaging [15, 16]. Here, an object is imaged using a pair of entangled photons, where one photon interacts with the object and only the other photon is measured. Notably, the photons can have different properties, such as belonging to different wavelength ranges. This is possible because the photon pair forms a composite state with a shared quantum phase. The phase that one photon acquires through its interaction with the object is transferred to the other photon through a method known as *path identity* [17, 18], which involves recombining superimposed paths of one of the photons.

In this paper, we introduce a novel setup that combines optical and matter wave interferometry in which an atom emits a photon at one of two possible locations (see Figure 1). Similar to Quantum Imaging, the phase accumulated by the atom is a common phase of the composite atom-photon state. By recombining the atomic paths at

the end of the interferometer, the phase previously accumulated by the atom is attributed to the coherent superposition, which is now assumed by the photon. The entire phase can then be read off from the photonic measurement, which allows conclusions to be drawn about the gravitational field. This is in contrast to state-of-the-art matter wave interferometry, where the phases of the matter waves are inferred from measurements of the atomic states.

In order to focus on the essentials, we reduce the setup described in this article to an idealized measurement scheme and discuss ideas for practical implementation further below in the article.

SETUP

Consider the setup depicted in Figure 1 in which a classical, point-like particle emits radiation in the positive z -direction while moving with a velocity v_0 along the x -direction, within a uniform gravitational field $\mathbf{g} = -g\mathbf{e}_z$. Alternatively, \mathbf{g} could also be treated as inertial acceleration, which would result in the same procedure. Radiation emitted at events **A** and **B** is directed into an interferometer, where it is recombined at a beam splitter before being measured. The time difference between events **A** and **B** of $2T_1$ results in a path difference traveled by the atom of $2gT_1^2$ downwards and $2v_0T_1$ in the x -direction. This path difference of the body results in an additional path for the radiation, denoted as δ . Consequently, a phase difference of $\Delta\Phi = 2\pi\frac{\delta}{\lambda} = \delta k$ arises, where λ represents the wavelength and k denotes the wave number of the radiation. Taking the difference between the intensities I^\pm recorded by the photodetectors **P**[−] and **P**⁺ and averaging over time yields

$$I^+ - I^- \propto \sin(-2kv_0T_1 + 2kgT_1^2 + \Delta\Phi_c), \quad (1)$$

where $\Delta\Phi_c$ contains the mirror and beam splitter phases. Here we have neglected all contributions of the order of magnitude $\mathcal{O}(v/c)$ and smaller. A more detailed derivation of this result can be found in the appendix.

Instead of a classical body we now consider a single atom with mass M emitting a single photon. Like be-

fore, the interference of the emitted photon at **A** and **B** is measured. The quantum state consists of photonic states and internal and center of mass degrees of freedom of the atom, which not only form a superposition but rather an entangled state. Quantum phases accumulated by the photon or atom are common phases of this entire entangled state. The idea of this setup is, that the quantum phase accumulated by the atom, which includes a gravitationally induced phase, is conveyed to the photonic states by recombining the atom's superimposed paths.

The structure of these states is illustrated in Figure 2. Consider the atom starting out with momentum $\hbar\mathbf{K}$ described by the center of mass state $|\mathbf{K}\rangle$ in an internally excited state $|e\rangle$ combined with no photons, which is described by $|0\rangle$. When combined, these states form a product state $|\mathbf{K}\rangle \otimes |e\rangle \otimes |0\rangle =: |\mathbf{K}, e; 0\rangle$. If the atom emits a photon at **A**, it does so by relaxing from the excited state to the ground state $|g\rangle$. The energy of the emitted photon is equal to the energy difference between the excited state and the ground state minus the change in the kinetic energy of the atom due to the recoil. The portion of the momentum of the atom that the photon takes is equal to $\hbar\mathbf{k}$, resulting in the product state $|\mathbf{K} - \mathbf{k}\rangle \otimes |g\rangle \otimes |a_{\mathbf{k}}\rangle =: |\mathbf{K} - \mathbf{k}, g; a_{\mathbf{k}}\rangle$, where $|a_{\mathbf{k}}\rangle$ describes a photon emitted at **A** with momentum \mathbf{k} . Here

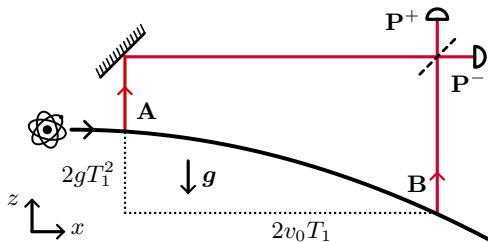


FIG. 1. Depicted is an overview of two possible interferometric setups.

a. A classical particle (solid black line) emitting radiation (red lines) is falling in a homogeneous gravitational field. The radiation emitted at **A** and at **B** is recombined on a beam splitter and measured by photodetectors labeled \mathbf{P}^- and \mathbf{P}^+ , while no further measurements are performed on the particle.
b. An atom (solid black line) is falling in a homogeneous gravitational field. The atom emits a single photon at two possible locations, **A** and **B**, with a time difference of $2T_1$, creating a state consisting of a coherent superposition of two paths (red lines) originating from those locations. For simplicity, the photon's recoil on the atom is not displayed in this diagram (see Fig. 2 for details). The photon's paths are then recombined on a beam splitter and subsequently measured, where again no further measurements are performed on the atom.

Information about the gravitational field can be obtained from the measurement results. The differences in the optical path length of the photons due to different emission events are indicated by the dotted lines.

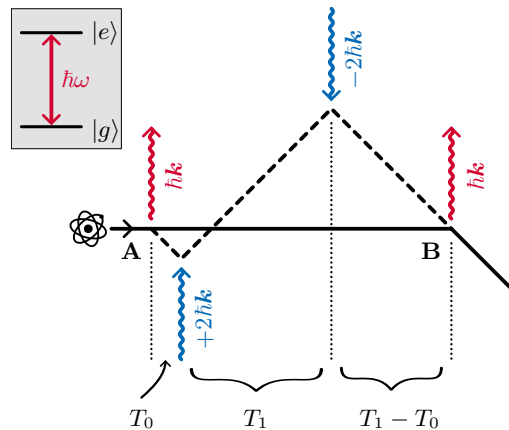


FIG. 2. Depicted are the possible paths of the atom in the atom's freely falling frame. The undisturbed path of the atom is illustrated as a solid black line. When spontaneously emitting a photon (red), the atom receives a recoil momentum $-\hbar\mathbf{k}$. If the atom emits the photon at location **A**, it alters its path, following the dashed black line. The dashed atom path is redirected twice using laser pulses (blue), which change the momentum by $\pm 2\hbar\mathbf{k}$ [19], ultimately recombining the atom's possible paths at location **B**.

we assume the photon emission to be instantaneous, that is, the emission duration is very short compared to the duration of the experiment. We further assume that the photon is emitted directly into the interferometer. This situation can be achieved by manipulating the emission process or by post-selection. Details can be found in the section about experimental aspects.

After the atom has passed **A**, we assume a 50/50 superposition of the initial state and the state after emission (more general emission amplitudes are discussed later)

$$|\Psi_A\rangle = \frac{1}{\sqrt{2}} \left(\int d^3k f(\mathbf{k}) |\mathbf{K} - \mathbf{k}, g; a_{\mathbf{k}}\rangle + |\mathbf{K}, e; 0\rangle \right), \quad (2)$$

where $f(\mathbf{k})$ describes the spectral and directional distribution of the photon. As one can easily verify, this state is entangled between the internal and center of mass degrees of freedom of the atom and the photonic state.

Next, two laser pulses (blue in Figure 2) are applied that only affect the atom if it has emitted a photon at **A**. As a result, this part of the trajectory of the atom is redirected so that it coincides with the atom's trajectory if it propagates freely to point **B** [20]. The emission process at **B** is assumed to be analogous to the emission process at **A** resulting in $\int d^3k f(\mathbf{k}) |\mathbf{K} - \mathbf{k}, g; b_{\mathbf{k}}\rangle$, which resembles the state of emission at **A**, but with a photonic state $|b_{\mathbf{k}}\rangle$ instead of $|a_{\mathbf{k}}\rangle$. $|b_{\mathbf{k}}\rangle$ also describes a photon with a sharply defined wave vector \mathbf{k} , but emitted at **B** and thus propagating along a different path.

Both parts of the atom's wave function superimpose at **B** with the same momentum and internal state, but

since they arrived via different paths, they have accumulated different quantum phases. These phases, along with phase contributions from the photons (e.g., due to reflection on the mirror), can be combined into Φ^A resp. Φ^B , which, in general, depend on the photon's wave vector. A detailed breakdown of $\Phi^{A/B}$ follows in the next section. The resulting state after recombination at \mathbf{B} can be expressed as

$$|\Psi_B\rangle = \frac{1}{\sqrt{2}} \int d^3k f(\mathbf{k}) e^{i\Phi^A(\mathbf{k})} |\mathbf{K} - \mathbf{k}\rangle \otimes |g\rangle \otimes \left(|a_{\mathbf{k}}\rangle + e^{i(\Phi^B(\mathbf{k}) - \Phi^A(\mathbf{k}))} |b_{\mathbf{k}}\rangle \right), \quad (3)$$

where we have used the previously mentioned *path identity*, i.e., that the internal and center of mass degrees of freedom of the atom are identical and can be factored out. In the following, the dependence of $\Phi^{A/B}$ on \mathbf{k} is not explicitly displayed. The final state as it arrives at the photodetectors \mathbf{P}^- and \mathbf{P}^+ can be calculated by applying the unitary beam splitter transformation

$$|a_{\mathbf{k}}\rangle \rightarrow \frac{1}{\sqrt{2}} (|P_{\mathbf{k}}^-\rangle + i|P_{\mathbf{k}}^+\rangle), \quad |b_{\mathbf{k}}\rangle \rightarrow \frac{1}{\sqrt{2}} (i|P_{\mathbf{k}}^-\rangle + |P_{\mathbf{k}}^+\rangle). \quad (4)$$

In order to obtain the probabilities for the measurement of a photon at \mathbf{P}^- or \mathbf{P}^+ , it is necessary to trace out the internal and center of mass degrees of freedom of the atom. Since $|\Psi_B\rangle$ in equation (3) is a product state, this results in the pure photonic state

$$|\Psi_{\text{ph}}\rangle = \frac{1}{2} \int d^3k f(\mathbf{k}) e^{i\Phi^A} \otimes \left[(1 + ie^{i\Delta\Phi}) |P_{\mathbf{k}}^-\rangle + (i + e^{i\Delta\Phi}) |P_{\mathbf{k}}^+\rangle \right], \quad (5)$$

where we have introduced the difference of the phases $\Delta\Phi := \Phi_B - \Phi_A$.

Assuming the detectors to be frequency insensitive, we obtain the probabilities

$$\mathcal{P}^\pm := \int d^3k |\langle P_{\mathbf{k}}^\pm | \Psi_{\text{ph}} \rangle|^2 = \frac{1}{2} \left(1 \pm \int d^3k |f(\mathbf{k})|^2 \sin(\Delta\Phi) \right), \quad (6)$$

where we used that $\int d^3k f(\mathbf{k}) = 1$. The detection probabilities can also be combined into a single value as $\mathcal{P}^+ - \mathcal{P}^- = \int d^3k |f(\mathbf{k})|^2 \sin(\Delta\Phi)$. This result is valid under the assumption, that half of the atom emits a photon at \mathbf{A} and the other half at \mathbf{B} . In order to also cover a more general case with arbitrary emission probabilities, an emission amplitude $|\alpha|$ is assumed for the emission at \mathbf{A} and an emission amplitude $|\beta|$ for the emission at \mathbf{B} . This modifies the result to

$$\mathcal{P}^+ - \mathcal{P}^- = 2|\alpha||\beta| \int d^3k |f(\mathbf{k})|^2 \sin(\Delta\Phi), \quad (7)$$

with $|a|^2 + |b|^2 = 1$, where the equality holds in the case that the atoms always emit a photon at either \mathbf{A} or \mathbf{B} . Importantly, $\Delta\Phi$ depends on the gravitational potential difference which can thus be inferred from measurements of (7).

In order to ensure that the influence of the gravitational acceleration \mathbf{g} is not averaged out we want to emphasize at this point that the width of the spectral distribution of the photon $f(\mathbf{k})$ must be small in comparison to $(gT_1^2)^{-1}$. For convenience the $|f(\mathbf{k})|^2$ is from now on assumed to be sufficiently narrow that the integral can be omitted and the phase terms are evaluated at a mean \mathbf{k} instead. Given that $k \propto E$, the assumption that the spectral distribution of the photon is narrow implies that the energy uncertainty of the emission process is small. With regard to the energy-time uncertainty principle, this is in contrast to the assumption, that emission duration (uncertainty) is also short. However, it is possible to briefly estimate that both assumptions can be satisfied simultaneously. Doing so leads to simple bounds on the experimental parameters, which are that $\frac{\Delta t}{T_1}$ has to be much larger than $v_0/2\pi c$, $(8\pi\omega_C T_1)^{-1/2}$ and $3gT_1/4\pi c$, with the Compton frequency $\omega_C = Mc^2/\hbar$, which usually assumes values between 10^{24} s^{-1} and 10^{27} s^{-1} .

DERIVATION OF THE PHASE

In the following, $\Phi^{A/B}$ will be calculated. The total interferometer phases as used in (7) consist of four components

$$\Phi^{A/B} = \Phi_{\text{at}}^{A/B} + \Phi_{\text{int}}^{A/B} + \Phi_{\text{ph}}^{A/B} + \Phi_{\text{c}}^{A/B} \quad (8)$$

with the atom's internal and center of mass degrees of freedom phase $\Phi_{\text{at}}^{A/B}$ and $\Phi_{\text{int}}^{A/B}$, respectively, the photonic phase $\Phi_{\text{ph}}^{A/B}$ and the constant phase contributions $\Phi_{\text{c}}^{A/B}$. This applies to both, the part of the atomic wave function emitting a photon at \mathbf{A} and the part emitting at \mathbf{B} . Since only the differences of these phases are of interest, it is sufficient to calculate $\Delta\Phi_i := \Phi_i^B - \Phi_i^A$ with $i \in \{\text{at}, \text{int}, \text{ph}, \text{const}\}$. In this derivation, all contributions of magnitude $\mathcal{O}(v/c)$ and smaller are neglected.

The simplest part of the total phase is given by the internal degrees of freedom of the atoms. Here we have

$$\Delta\Phi_{\text{int}} = -2\omega T_1, \quad (9)$$

since during the time in the interferometer, the two different parts of the atomic wave function are continuously in different energy levels.

For the photonic phase component, the optical path difference between photons emitted at \mathbf{A} and photons emitted at \mathbf{B} must be considered and is given by $\Delta\Phi_{\text{ph}} = k\delta$, with the aforementioned path difference δ . As can be seen in Figure 1, a photon emitted at \mathbf{A} has an additional travel distance of $2v_0T_1$, with the initial velocity

in x -direction v_0 , and a photon emitted at \mathbf{B} has to additionally travel the distance $2gT_1^2$. Together with the photon's temporal evolution, this results in

$$\Delta\Phi_{\text{ph}} = 2\omega T_1 - 2kv_0T_1 + 2kgT_1^2. \quad (10)$$

Until now, all derived phase terms had a classical counterpart. This changes when considering the center of mass degrees of freedom of the atom quantum mechanically. It is here where the similarity to Quantum Imaging occurs, with the atom corresponding to the idler photon shown in [15], also establishing what is called *path identity* in later articles. The derivation of the atom phase is performed similarly as described in [21] by calculating

$$\Phi_{\text{at}}^{\text{A/B}} = \frac{1}{\hbar} \int_0^T \mathcal{L}^{\text{A/B}} dt, \quad (11)$$

where T is the travel time of the atom between the two emission events, i.e. \mathbf{A} and \mathbf{B} in Figure 2. \mathcal{L}^{B} represents the classical Lagrangian of atoms following the solid line and \mathcal{L}^{A} the classical Lagrangian of atoms following the dashed line. Accordingly, for this setup, we have $T = 2T_1$. The integrals are carried out along the atom's classical path. While it may seem natural to perform the calculations in the laboratory frame, it turns out to be easier to do so in the freely falling frame of the atom, since the gravitational acceleration then occurs exclusively in the laser pulse terms. The Lagrangians expressed in such a frame can be written as

$$\mathcal{L}^{\text{A}} = \frac{M}{2} [\dot{x}^2 + \dot{z}^2] - V_{\text{SE}}^{\text{A}} - V_{\text{laser}}^{\text{A}}, \quad (12)$$

$$\mathcal{L}^{\text{B}} = \frac{M}{2} [\dot{x}^2 + \dot{z}^2] - V_{\text{SE}}^{\text{B}}, \quad (13)$$

where \dot{z} represents the atom's velocity in the direction (anti-)parallel to gravity, and \dot{x} the velocity in the atom's initial direction perpendicular to \mathbf{g} . $V_{\text{SE}}^{\text{A/B}}$ denotes the potentials due to the recoil induced by the spontaneous emission of a photon at either \mathbf{A} or \mathbf{B} and $V_{\text{laser}}^{\text{A}}$ represents the potential due to the laser kicks, which exclusively applies to the part of the atomic wave function emitting at \mathbf{A} . The effective potential due to the laser light is given by [21]

$$V_{\text{laser}}^{\text{A}} = -2\hbar k \left(z + \frac{1}{2}gt^2 \right) \times (\delta(t - T_0) - \delta(t - T_0 - T_1)), \quad (14)$$

where it is assumed that $\mathbf{k} \parallel \mathbf{e}_z$. Here, the term $+\frac{1}{2}gt^2$ arises from the fact that, in the freely falling frame of the atom, the laser is accelerated upwards by g . Similarly, the potential due to the spontaneous emission of photons and the associated recoil is introduced as [22]

$$V_{\text{SE}}^{\text{A}} = +\hbar k z \delta(t), \quad V_{\text{SE}}^{\text{B}} = +\hbar k z \delta(t - 2T_1), \quad (15)$$

with k being the wave number of the photon. It is important to note that, although the δ -distributions in (15) are centered at the edges of the integral in (11), we consider them to lie completely within the integration interval. This is a reasonable assumption since we could extend the time integral on both sides without altering the result.

Now in order to calculate the integrals in (11), we first need the classical paths for the atom which we can readily obtain by plugging (13) and (12) into the Euler-Lagrange equation. Since the result depends only on relative velocities and not on the absolute choice of a coordinate system, we can, without loss of generality, set for this calculation $x(0) = \dot{x}(0) = z(0) = \dot{z}(0) = 0$. Afterwards, evaluating (11) is straight forward and results in a phase difference of

$$\Delta\Phi_{\text{at}} = \frac{\hbar k^2}{M} T_1 + kgT_1(2T_0 + T_1) \quad (16)$$

Here $\frac{\hbar k^2}{M} T_1$ represents the kinetic energy due to the photonic recoil. The important term is $kgT_1(2T_0 + T_1)$, which is proportional to the gravitational acceleration.

It is convenient to gather all unknown but constant phase contributions due to the photon emission processes, the interaction of the laser pulses with the atom, as well as numerous further sources of constant phase shifts due to optical elements, such as mirrors, beam splitters, lenses, etc. into one term resulting in the constant phase difference $\Delta\Phi_{\text{c}}$.

By substituting 9, 10 and 16 into 7, we obtain

$$\mathcal{P}^+ - \mathcal{P}^- = 2|\alpha||\beta| \sin \left(-2kv_0T_1 + \frac{\hbar k^2}{M} T_1 + kgT_1(2T_0 + 3T_1) + \Delta\Phi_{\text{c}} \right). \quad (17)$$

Since the $\Delta\Phi_{\text{c}}$ term in this result is unknown, a single absolute measurement of $\mathcal{P}^+ - \mathcal{P}^-$ provides no information about the gravitational acceleration. One approach to obtain information on \mathbf{g} would be to vary the delay T_0 in several measurements while keeping the total duration $2T_1$ constant. In this way, the part of the atomic wave function that has emitted a photon at point \mathbf{A} could be deflected, providing the desired information.

To achieve maximum contrast, the coefficient $|\alpha||\beta|$ in (17) must be maximized under the additional condition $|\alpha|^2 + |\beta|^2 = 1$. As briefly mentioned before, this is the case for $|\alpha| = |\beta| = \frac{1}{\sqrt{2}}$, i.e., when the emission probability for a photon is 50% each for both emission events.

EXPERIMENTAL ASPECTS

In the derivation presented in this article, several shortcuts have been employed, which here shall be discussed in more detail.

Firstly, it must be taken into account that both the atomic and photonic wave functions are not point like, but have spatial extensions. Moreover, the recoil of the photon does not have a single associated momentum, but rather a momentum distribution, coupled with a distribution in the time domain. This leads to further broadening of the atomic wave function. Care must be taken to ensure that this broadening remains sufficiently small compared to the path deviation of the atom due to the photonic recoil; otherwise, the quantity we want to measure might be diminished. A viable approach to address this would be to model the wave functions involved microscopically within the framework of the Wigner-Weisskopf theory of spontaneous emission. This would also help answering the questions raised in the previous chapters regarding the phase relation between the two parts of the wave function.

Another assumption made in the derivation was that the photon is emitted only at two specific events on the atom's trajectory and only in one specific direction. While this condition can be achieved by post-selecting only those photons that fulfill these criteria, doing so would result in a very low data rate and thus be hard to measure. Two possibly better methods are:

- Utilizing an atom in a third, dark state, one that does not relax over the course of the experiment. Initially, at the first emission event, half of the atom is pumped into the excited state (e.g. by using a resonant $\pi/2$ -pulse), which relaxes immediately and emits a photon. Subsequently, at the second emission event, the remaining half of the atom in the dark state is pumped into the excited state, again leading to relaxation and photon emission. As with the laser pulses described in this article, these pump pulses would introduce additional gravitationally dependent phase changes to the atom, thus altering the g -dependent term in 17. Also, the direction of emission can be controlled by aligning the atom's dipole moment.
- Leveraging the Purcell effect by placing cavities at the positions where the photons should be emitted would not only increase the emission probability at these events but also enhance emission in the desired direction.

Finally, the optical part of the interferometer needs to be addressed in more detail. This would involve, among other things, introducing a delay for the first emitted photon so that it can recombine simultaneously at the beam splitter with the second emitted photon. However, any constant phases that arise on the paths of the photons can be attributed to the phase of the photon emission process, which was assumed to be unknown anyways.

CONCLUSIONS

In conclusion, we have introduced a method with the potential for high-precision measurement of the gravitational field based on Quantum Imaging. Since we consider individual atoms in our setup, we benefit from the same advantages as atomic interferometry, such as high reproducibility and the potential for high-precision gravitational measurements. Moreover, our approach adds a novel twist as the information of the gravitational field is completely encoded in the state of the emitted photons.

In our current derivation, we assume a homogeneous gravitational field, thus limiting our measurements to gravitational and inertial acceleration. Future work could extend this model to include curvature or the multipole moments of the gravitational potential, thereby enhancing its applicability in geodesy. Although the assumptions and approximations made in this article are reasonable to demonstrate the feasibility of our setup, high-precision measurements and the aforementioned extensions may require more rigorous calculations. As briefly mentioned throughout the article, this would involve considering a distribution of the photon's wave vector, which in turn leads to a distribution of the atom's momentum. Addressing this requires a microscopic treatment of the derivation. Apart from geodesic applications, the presented setup is also interesting for studying the fundamental interface between quantum mechanics and gravitation, as we consider entanglement between two completely different kinds of particles.

ACKNOWLEDGMENTS

We gratefully acknowledge Emanuel Schlake and Jan P. Hackstein for fruitful discussions on the topic. M.C. acknowledges funding by the CRC TerraQ from the Deutsche Forschungsgemeinschaft (DFG, German Research Foundation) – Project-ID 434617780 – SFB 1464. D.R. acknowledges funding by the Federal Ministry of Education and Research of Germany in the project “Open6GHub” (grant number: 16KISK016) and support by the Deutsche Forschungsgemeinschaft (DFG, German Research Foundation) under Germany's Excellence Strategy – EXC-2123 QuantumFrontiers – 390837967.

-
- [1] M. A. Kasevich and S. Chu. Measurement of the gravitational acceleration of an atom with a light-pulse atom interferometer. *Applied Physics B Photophysics and Laser Chemistry*, 54(5):321–332, May 1992.
- [2] A. Peters, K. Y. Chung, and S. Chu. Measurement of gravitational acceleration by dropping atoms. *Nature*, 400(6747):849–852, August 1999.

- [3] V. Ménotet, P. Vermeulen, N. Le Moigne, S. Bonvalot, P. Bouyer, A. Landragin, and B. Desruelle. Gravity measurements below 10-9 g with a transportable absolute quantum gravimeter. *Scientific Reports*, 8(1):12300, August 2018.
- [4] Z.-K. Hu, B.-L. Sun, X.-C. Duan, M.-K. Zhou, L.-L. Chen, S. Zhan, Q.-Z. Zhang, and J. Luo. Demonstration of an ultrahigh-sensitivity atom-interferometry absolute gravimeter. *Physical Review A*, 88(4):043610, October 2013.
- [5] G. W. Biedermann, X. Wu, L. Deslauriers, S. Roy, C. Mahadeswaraswamy, and M. A. Kasevich. Testing gravity with cold-atom interferometers. *Physical Review A*, 91(3):033629, March 2015.
- [6] R. P. Del Aguila, T. Mazzoni, L. Hu, L. Salvi, G. M. Tino, and N. Poli. Bragg gravity-gradiometer using the $^1\text{S}_0 - ^3\text{P}_1$ intercombination transition of ^{88}Sr . *New Journal of Physics*, 20(4):043002, April 2018.
- [7] D. Schlippert, J. Hartwig, H. Albers, L. L. Richardson, C. Schubert, A. Roura, W. P. Schleich, W. Ertmer, and E. M. Rasel. Quantum Test of the Universality of Free Fall. *Physical Review Letters*, 112(20):203002, May 2014.
- [8] M. G. Tarallo, T. Mazzoni, N. Poli, D. V. Sutyryn, X. Zhang, and G. M. Tino. Test of Einstein Equivalence Principle for 0-Spin and Half-Integer-Spin Atoms: Search for Spin-Gravity Coupling Effects. *Physical Review Letters*, 113(2):023005, July 2014.
- [9] P. Asenbaum, C. Overstreet, M. Kim, J. Curti, and M. A. Kasevich. Atom-interferometric test of the equivalence principle at the 10^{-12} level. *Physical Review Letters*, 125:191101, Nov 2020.
- [10] H. Müller, S.-W. Chiow, S. Herrmann, S. Chu, and K.-Y. Chung. Atom-Interferometry Tests of the Isotropy of Post-Newtonian Gravity. *Physical Review Letters*, 100(3):031101, January 2008.
- [11] S. Dimopoulos, P. W. Graham, J. M. Hogan, M. A. Kasevich, and S. Rajendran. Atomic gravitational wave interferometric sensor. *Physical Review D*, 78(12):122002, December 2008.
- [12] C. K. Hong, Z. Y. Ou, and L. Mandel. Measurement of subpicosecond time intervals between two photons by interference. *Physical Review Letters*, 59(18):2044–2046, November 1987.
- [13] R. Lopes, A. Imanaliev, A. Aspect, M. Cheneau, D. Biron, and C. I. Westbrook. Atomic Hong–Ou–Mandel experiment. *Nature*, 520(7545):66–68, April 2015.
- [14] X. Y. Zou, L. J. Wang, and L. Mandel. Induced coherence and indistinguishability in optical interference. *Physical Review Letters*, 67(3):318–321, July 1991.
- [15] G. B. Lemos, V. Borish, G. D. Cole, S. Ramelow, R. Lapkiewicz, and A. Zeilinger. Quantum imaging with undetected photons. *Nature*, 512(7515):409–412, August 2014.
- [16] M. Gilaberte Basset, F. Setzpfandt, F. Steinlechner, E. Beckert, T. Pertsch, and M. Gräfe. Perspectives for Applications of Quantum Imaging. *Laser & Photonics Reviews*, 13(10):1900097, October 2019.
- [17] M. Lahiri. Many-particle interferometry and entanglement by path identity. *Physical Review A*, 98(3):033822, September 2018.
- [18] A. Hochrainer, M. Lahiri, M. Erhard, M. Krenn, and A. Zeilinger. Quantum indistinguishability by path identity and with undetected photons. *Reviews of Modern Physics*, 94(2):025007, June 2022.
- [19] E. Giese, A. Roura, G. Tackmann, E. M. Rasel, and W. P. Schleich. Double Bragg diffraction: A tool for atom optics. *Physical Review A*, 88(5):053608, November 2013.
- [20] Ideas on how this could be implemented in practice are discussed in the discussions.
- [21] W. P. Schleich, D. M. Greenberger, and E. M. Rasel. A representation-free description of the Kasevich–Chu interferometer: A resolution of the redshift controversy. *New Journal of Physics*, 15(1):013007, January 2013.
- [22] A derivation of this potential can be found in the appendix.
- [23] M. O. Scully and M. S. Zubairy. *Quantum Optics*. Cambridge University Press, 1 edition, September 1997.

Classical derivation

A derivation of the classical radiation phase, as shown at the beginning of this article, is presented in more detail here. Since we are only interested in radiation emitted in (positive) z -direction, the emitted electrical field can be regarded as

$$\mathbf{E}(t, \mathbf{r}) = \mathbf{E}_0 \cos(k(z - z_0) - \omega t + \varphi), \quad (18)$$

where \mathbf{E}_0 is the amplitude of the electrical field perpendicular to \mathbf{e}_z , k the wave number of the radiation and ω is the corresponding frequency connected by $\omega = ck$ with c being the velocity of light. φ represents some arbitrary but constant phase offset. z_0 denotes a spatially offset which in our case contains the extra distance the radiation emitted at \mathbf{B} has to travel (not only in z -direction, but also in x -direction) compared to the radiation emitted at \mathbf{A} . Since the radiating body oscillates in phase with the radiation it emits, there is no temporal offset between the radiation emitted at \mathbf{A} and \mathbf{B} . Plugging in the values for this case yields

$$\mathbf{E}^{\text{A}}(t, \mathbf{r}) = \mathbf{E}_0 \cos(kz - \omega t + \varphi_{\text{A}}) \quad (19)$$

$$\mathbf{E}^{\text{B}}(t, \mathbf{r}) = \mathbf{E}_0 \cos(k(z - 2v_0T_1 + 2gT_1^2) - \omega t + \varphi_{\text{B}}) \quad (20)$$

Here we assumed two different phase offsets, which account for the different paths the radiation takes. The detectors measure the intensity of the radiation, which is proportional to the square of the electrical field averaged over time, i.e.,

$$I^{\pm} \propto \lim_{T \rightarrow \infty} \frac{1}{T} \int_0^T (\mathbf{E}^{\pm}(t, \mathbf{r}))^2 dt. \quad (21)$$

The electrical field in this formula represents a linear combination of \mathbf{E}^{A} and \mathbf{E}^{B} with the phase of the electrical field which was reflected at a 50:50 beam splitter shifted by $+\pi/2$. Evaluating this for both detectors and calculating the difference gives (1) where the phase difference $\Delta\Phi_c = \varphi_{\text{B}} - \varphi_{\text{A}}$ was introduced and coefficients were omitted.

Derivation of spontaneous emission potential

We begin our derivation with the state evolution that results from the Wigner-Weisskopf theory of spontaneous emission, which can be found, for example, in [23], and reads

$$|\Psi(t)\rangle = e^{-\frac{\Gamma}{2}t} |e, 0\rangle + \sum_{\mathbf{k}} \alpha_{\mathbf{k}} e^{-i\mathbf{k}\cdot\mathbf{r}_0} \left[\frac{1 - e^{i\Delta_k t - \frac{\Gamma}{2}t}}{-\Delta_k + i\frac{\Gamma}{2}} \right] |g, \mathbf{1}_{\mathbf{k}}\rangle. \quad (22)$$

Here Γ represents the decay constant, \mathbf{r}_0 the location of the atom, $\Delta_k = \omega - ck$ the detuning and $\alpha_{\mathbf{k}} = \frac{\mathcal{E}_{\mathbf{k}} \mathbf{D}\cdot\boldsymbol{\varepsilon}_{\mathbf{k}}}{\hbar}$ a generally complex factor, with the dipole moment \mathbf{D} , the polarization direction $\boldsymbol{\varepsilon}_{\mathbf{k}}$ and a normalization constant $\mathcal{E}_{\mathbf{k}}$. In this calculation, it is assumed that the position of the atom is constant, which is justified by the assumption that the emission process is very short.

The term $\frac{1}{-\Delta_k + i\frac{\Gamma}{2}}$ is characteristic of relaxation processes and describes a Lorenz-distributed spectrum centered at $\Delta_k = 0$ with a width of Γ . To keep this derivation simple, we replace the sum over \mathbf{k} by the peak value of the Lorenz curve $\Delta_{k_0} = 0$, i.e. $\mathbf{k}_0 = \frac{\omega}{c} \mathbf{e}_z$. A similar assumption is made when deriving the Wigner-Weisskopf theory. Note that the application of this approximation leads to a non-normalized state, as we omit parts of the state. This will be corrected later. Here we choose \mathbf{k}_0 so that it points in the z -direction, since these are the photons we are interested in. Normally, the emission direction is determined by $\alpha_{\mathbf{k}}$ or more precisely by $\mathbf{D}\cdot\boldsymbol{\varepsilon}_{\mathbf{k}}$ which would, e.g. for S-orbitals, emit equally in all directions. A more detailed discussion of the emission direction can be found in the article.

The resulting state is

$$|\Psi(t)\rangle = e^{-\frac{\Gamma}{2}t} |e, 0\rangle + \alpha_{\mathbf{k}_0} e^{-i\mathbf{k}_0 z_0} \frac{1 - e^{-\frac{\Gamma}{2}t}}{i\frac{\Gamma}{2}} |g, \mathbf{1}_{\mathbf{k}_0}\rangle. \quad (23)$$

We can now divide the complex factor into modulus and phase terms $\alpha_{\mathbf{k}_0} \frac{1 - e^{-\frac{\Gamma}{2}t}}{i\frac{\Gamma}{2}} = \beta e^{-i\varphi}$ and replace the real coefficient $e^{-\frac{\Gamma}{2}t} = \gamma$ which results in $|\Psi(t)\rangle = \beta |e, 0\rangle + \gamma e^{-i\varphi} e^{-i\mathbf{k}_0 z_0} |g, \mathbf{1}_{\mathbf{k}_0}\rangle$. As already mentioned we will have $\beta^2 + \gamma^2 \leq 1$ due to the approximations made before. Since the final state must be normalized after spontaneous emission, we can correct this side effect of our previous approximation by setting $\beta = \sqrt{1 - \gamma^2}$. Finally, we obtain

$$|\Psi(t)\rangle = \sqrt{1 - \gamma^2} |e, 0\rangle + \gamma e^{-i\mathbf{k}_0 z_0 - i\varphi} |g, \mathbf{1}_{\mathbf{k}_0}\rangle. \quad (24)$$

Here, $\gamma = \gamma(t)$ and $\varphi = \varphi(t)$ are time-dependent. For γ we can conclude that $\gamma(0) = 0$ and $\lim_{t \rightarrow \infty} \gamma(t) = 1$.

Finally, to derive the potential for spontaneous emission, we first assume that the emission is instantaneous, i.e. $\Gamma \rightarrow \infty$. In this case, $\gamma(t)$ becomes a step function,

and the action of the potential can be restricted to an infinitesimally short time period represented by the Dirac delta distribution $\delta(t)$, leading to a model of the potential that is

$$V_{SE} = \hbar [kz(t) + \varphi(t)] \delta(t - T), \quad (25)$$

where T is the time at which the emission takes place. As in [21], we can construct a Hamiltonian with this potential $H_{SE} = \frac{p^2}{2M} + V_{SE}$ and neglect the kinetic part. This allows us to calculate the state directly after the emission by applying the time evolution operator to a state directly before the emission

$$|\Psi(T + \delta)\rangle = \exp\left(-\frac{i}{\hbar} \int_{T-\delta}^{T+\delta} V_{SE} dt\right) |\Psi(T - \delta)\rangle, \quad (26)$$

$$= e^{-ikz(T) - i\varphi(T)} |\Psi(T - \delta)\rangle. \quad (27)$$

A comparison with the last part of (24) shows that this potential actually corresponds to our earlier description of spontaneous emission.

For the article, we omit the term $\varphi(t)$ that we calculated in (25), since it is independent of position and momentum. Such a term corresponds to an arbitrary potential offset, which vanishes when dealing with classical Euler-Lagrange equations, as we do here. These phase terms are assumed to be constant throughout the experiment and are collectively reintroduced at a later time together with other constant phase contributions.

Energy-time uncertainty principle

In (7), we assumed that the wave number spectrum of the photon is narrow compared to the inverse of the distance traveled by the atom. Otherwise, the integral would remain in (17). If the spectrum width, denoted as Δk , were large, the dependence on g would average out. This implies that the terms within the sine function in (17), with k replaced by Δk , must be small compared to 2π . Consequently, we obtain three inequalities: $2\Delta k v_0 T_1 \ll 2\pi$, $\frac{\hbar \Delta k^2}{M} T_1 \ll 2\pi$, and $3\Delta k g T_1^2 \ll 2\pi$, where we have focused on the leading term in the last inequality. Furthermore, the energy-time uncertainty principle holds, which states $c\Delta k \Delta t \geq \frac{1}{2}$, of which we use the lower bound. Combining these inequalities results in the following conditions:

$$\frac{\Delta t}{T_1} \gg \frac{v_0}{2\pi c}, \quad (28)$$

$$\frac{\Delta t}{T_1} \gg \frac{1}{2c} \sqrt{\frac{\hbar}{2\pi M T_1}} = \frac{1}{\sqrt{8\pi\omega_C T_1}}, \quad (29)$$

$$\frac{\Delta t}{T_1} \gg \frac{3g T_1}{4\pi c}, \quad (30)$$

where we introduce the Compton frequency ω_C . (28) and (30) suggest that the lower bound for Δt is sufficiently

small if $v_0 \ll c$ or $gT_1 \ll c$, respectively, indicating a non-relativistic regime, as assumed in this article. (29) results in a small lower bound if $T_1 \gg \omega_C^{-1}$, which is fulfilled in consideration of the extremely large Compton frequency ω_C for atoms.

By inserting explicit values [6], we can estimate the order of magnitude of these bounds. Assuming ^{88}Sr as the

atom species and experimental values of $v_0 = 1 \text{ mm/s}$, $T_1 = 0.1 \text{ s}$, and $g = 9.81 \text{ m/s}^2$, we find that the largest lower bound for the emission time is given by (30), approximately $\Delta t \gg 8 \cdot 10^{-11} \text{ s}$. We also required in the article $\Delta t \ll 2T_1$, which can easily be fulfilled simultaneously with the bounds derived before.